Force Generation and Work Production by Covalently Cross-Linked Actin-Myosin Cross-Bridges in Rabbit Muscle Fibers

S. Y. Bershitsky and A. K. Tsaturyan
The Randall Institute, King's College London, London WC2B 5RL, United Kingdom

ABSTRACT To separate a fraction of the myosin cross-bridges that are attached to the thin filaments and that participate in the mechanical responses, muscle fibers were cross-linked with 1-(3-dimethylaminopropyl)-3-ethylcarbodiimide and then immersed in high-salt relaxing solution (HSRS) of 0.6 M ionic strength for detaching the unlinked myosin heads. The mechanical properties and force-generating ability of the cross-linked cross-bridges were tested with step length changes (L-steps) and temperature jumps (T-jumps) from 6–10°C to 30–40°C. After partial cross-linking, when instantaneous stiffness in HSRS was 25–40% of that in rigor, the mechanical behavior of the fibers was similar to that during active contraction. The kinetics of the T-jump-induced tension transients as well as the rate of the fast phase of tension recovery after length steps were close to those in unlinked fibers during activation. Under feedback force control, the T-jump initiated fiber shortening by up to 4 nm/half-sarcomere. Work produced by a cross-linked myosin head after the T-jump was up to 30×10^{-21} J. When the extent of cross-linking was increased and fiber stiffness in HSRS approached that in rigor, the fibers lost their viscoelastic properties and ability to generate force with a rise in temperature.

INTRODUCTION

It is widely believed that myosin cross-bridges produce muscle force interacting with actin. However, it is difficult to distinguish force-generating processes in attached cross-bridges from the effects of the reattachment of detached cross-bridges during normal muscle contraction. Evidence for fast cross-bridge reattachment after a step change in length was obtained recently in mechanical (Lombardi et al., 1992) and x-ray (Irving et al., 1992) experiments.

A procedure was developed to prevent cross-bridge attachment to and their detachment from actin. Myosin heads in permeabilized muscle fibers were covalently cross-linked to actin with a zero-length linker, 1-(3-dimethylaminopropyl)-3-ethylcarbodiimide (EDC), and then immersed in a high-salt relaxing solution (HSRS) of 0.6 M ionic strength in which all unlinked myosin heads are detached from actin. In this solution, only cross-linked myosin heads contribute to the mechanical behavior of the muscle fibers. Tawada and Kimura (1986) have shown that EDC initially cross-links myosin rods so that the fibers can be immersed in HSRS of up to 1 M ionic strength without dissolving the myosin filaments. The cross-linked fibers in HSRS have been shown to produce work during small-amplitude length oscillations (Tawada and Kawai, 1990). Force is generated when the fibers are transferred from HSRS into rigor solution (Tawada et al., 1989). It is difficult, however, to study the force-generating ability of cross-linked muscle fibers in pure mechanical experiments.

With the joule temperature jump (T-jump) technique, fiber temperature can be increased from 5–10°C up to 40°C in 0.15 ms (Bershitsky and Tsaturyan, 1989, 1992). Such a temperature rise causes a severalfold increase in tension with a relatively small increase in stiffness during fully activated isometric contraction. This shows that force-generating processes are involved in the muscle response to the T-jump, and hence, the T-jump can be used for initiation of the power stroke in cross-linked cross-bridges. To measure fiber stiffness and estimate viscoelastic properties of the cross-linked bridges, tension responses to step length changes (L-steps) were studied in the cross-linked fibers and compared with those before cross-linking.

MATERIALS AND METHODS

Muscle fiber preparation

Dutch gray rabbits (3–3.5 kg) were killed by intravenous injection of sodium pentobarbitone. Bundles of muscle fibers of approximately 2 mm in diameter and 3 cm long were dissected from psoas minor muscle and tied to wooden sticks at slack length. Each bundle was put into a 5-ml plastic tube filled with storage solution (containing in mM: 5 ATP, 6 $MgCl_2$, 5 EGTA, 40 potassium proprionate, 80 imidazole, pH 7.0, at 25°C and 50% (v/v) glycerol) and kept at −20°C for 24 h. The solution was replaced and the bundles were stored at −20°C for up to 2 months. The bundles used during the first week were immersed in the storage solution with 0.5–1% (v/v) Triton X-100 for 1–2 h before use.

Single muscle fibers were dissected in the storage solution with fine forceps. A fiber was placed onto a glass coverslip with a drop of the same solution and transferred to the experimental trough. A 2 ± 0.2-mm-long fiber segment in air at 5°C was glued to the nickel tubing ends of the length motor and of the force transducer with shellac dissolved in ethanol (~50% w/v) and then let down into the trough with relaxing solution. Sarcomere length was adjusted by laser diffraction to be 2.4–2.5 μm. Fiber width was then measured in both solution and air in two perpendicular directions with a dissecting microscope and dividing prism (Bershitsky and Tsaturyan, 1992).

Received for publication 10 January 1995 and in final form 6 June 1995.
Address reprint requests to Dr. Andrey K. Tsaturyan, Institute of Mechanics, Moscow University, 1 Mitchurinsky Prospect, Moscow 117192 Russia. Tel.: 011-095-939-1252; Fax: 011-095-292-6511, box 570; E-mail: tsat@inmech.msu.su.

0006-3495/95/09/1011/11 $2.00

EDC cross-linking

The procedure described by Tawada and Kimura (1986) was used with some modifications. A fiber was put into rigor at 0°C in the experimental trough. Rigor solution (5 mM EDTA, 50 mM potassium propionate, 80 mM imidazole, pH 7.0, at 25°C) was replaced two or three times and the fiber was kept at this temperature for at least 10 min before raising it to 15°C. The rigor solution was replaced again and the fiber was incubated for an additional 10 min. Such a rigorizing procedure brought the fiber into rigor with minimal disorder of the sarcomere lengths. The fiber was immersed in a buffer solution (50 mM KCl, 80 mM imidazole, pH 7.0, at 25°C) for 10–15 min and then in the cross-linking solution (the same buffer plus 15 mM EDC) for 15–120 min. To prevent a possible cross-linking of any parallel (non-cross-bridge) structures, the fiber was stretched and released by approximately 0.5% of its length every 3 s during the cross-linking procedure. Excessive cross-linking was stopped by rinsing the trough twice with the buffer solution.

In most cases, the experiments with cross-linked fibers were made with rigor and relaxing solutions the ionic strength of which was increased to 0.6 M. HSRS contained (in mM): 5 ATP, 6.5 $MgCl_2$, 10 EGTA, 15 creatine phosphate, 100–150 U/ml phosphocreatine kinase, 435 potassium propionate, 100 cacodylic acid, pH 7.0, at 25°C. High-salt rigor solution contained (in mM): 10 EDTA, 480 potassium propionate, 100 cacodylic acid, pH 7.0. Activating solution contained (in mM): 5 ATP, 6.5 $MgCl_2$, 10 Ca-EGTA, 15 creatine phosphate, 100–150 U/ml phosphocreatine kinase, 100 cacodylic acid, pH 7.0. Cacodylic was chosen as a pH buffer because of its low temperature coefficient ($\Delta pK_a/\Delta T = -0.0045\ K^{-1}$; Bershitsky and Tsaturyan, 1992). The degree of EDC cross-linking was estimated by fiber stiffness in HSRS compared with that in rigor solution.

ATPase in EDC cross-linked fibers was measured at 15°C by the method of Glyn and Sleep (1985). A fiber trough of 100-μl volume was filled with HSRS containing additionally 0.1 mM NADH, 10 mM phosphoenolpyruvate, 1 mg/ml L-lactate dehydrogenase from rabbit muscle type II (950 U/mg), and 10 mg/ml pyruvate kinase from rabbit muscle type II (500 U/mg). After the muscle fiber was immersed in this solution for 1 h, the solution from the trough was mixed with 400 μM of the same solution and then light absorption at 340 nm was compared with that of the control sample.

Temperature jump

The principle of the joule temperature jump (T-jump) method was described before (Bershitsky and Tsaturyan, 1992). Briefly, a high-voltage (up to 5 kV) AC (40 kHz) current pulse of 0.15 ms duration was passed through a muscle fiber suspended in air. The amplitude of the T-jump was calculated by dividing the pulse energy by the fiber's thermal capacity. The power was obtained as the product of the pulse voltage and current. The energy was calculated as an integral of the power. In the present study, the fiber temperature was kept nearly constant after the T-jump by an AC pulse of a smaller amplitude and 0.2 s duration to compensate for fiber cooling.

Adjustment of the warming pulse

The amplitude of the warming pulse was adjusted by monitoring the temperature time course in a fiber. For this, in a control experiment, we recorded absorption of He-Ne laser light in a muscle fiber immersed in relaxing solution containing 100 mM of the thermosensitive ($\Delta pK_a/\Delta T = -0.027\ K^{-1}$) Tris buffer (pH 7.8) and bromthymol blue pH-sensitive dye in saturated concentration (both from Sigma Chemical Co., St. Louis, MO). A good correspondence was found between the temperature of this solution measured in the trough by a miniature thermometer and its light absorption in the temperature range of 0–40°C. The dyed relaxed fiber was suspended in air at 6°C and T-jumps to 30–35°C were applied. Records of changes in the fiber temperature made by this method were rather noisy because of the short optical path in the fiber; however, the kinetics of fiber cooling could be analyzed reasonably well. The amplitude of the warming pulse was adjusted to maintain the output light signal as constant as possible for 200 ms after the T-jumps. When the T-jump magnitude was changed, the warming pulse amplitude was scaled proportionally. It has been shown previously (Bershitsky and Tsaturyan, 1992) that heat and vapor diffusion from the fiber surface after T-jumps in air are the main cooling mechanisms and the apparent rate constant of the fiber cooling is in inverse proportion to the square of the fiber diameter. In additional experiments, the amplitude of warming pulses was chosen by using this ratio.

Mechanical set-up

Trough and temperature control

The experimental trough was an aluminium block consisting of two 2.5-mm-thick walls covered by a thin layer of silicon rubber. The walls (10 mm long and 15 mm high) were 2 mm apart, forming a gap trough. In the lower part of the trough, 100 μl of solution was kept by surface tension. The air gap above the solution surface was broad enough to prevent sparking of the high voltage (up to 5 kV) heating pulse. Temperature in the air part of the trough was 5°C when solution temperature was 0°C and room temperature was 20–25°C. A miniature (~0.5 mm diameter) bare transistor used as a thermometer was incorporated into the trough wall for temperature feedback control. The same thermometer, but covered with a thin layer of silicon rubber, was placed into the trough close to the fiber for monitoring temperature when the fiber was either in solution or in air. The trough was mounted on an assembly of 5-W and 15-W Peltier heat pumps (Farnell Electronic Components, Leeds, UK), which maintained temperature in the range of 0–40°C with an accuracy of 0.2 K under feedback control. This assembly was placed onto a microscope manipulator providing up-and-down displacement. In the lower position, the fiber was immersed in solution, whereas in the upper position it was suspended in air between the trough walls where the fiber contacted neither walls nor solution and the electrical pulse for the T-jump could be applied. The laser beam passed through one of two pairs of elliptical (2.5 × 6 mm) holes in the walls. The lower pair of holes was glassed and used when the fiber was in solution. When the fiber was in air, the beam passed through the upper holes.

Sarcomere length control

A laser diffractometer designed by Dr. K. Burton was used with some modifications. A 5-mW He-Ne laser and a position-sensitive photodiode (LSC/30D; United Detector Technology, Hawthorne, CA) were used for sarcomere length monitoring and control. The laser beam was focused on the fiber over a range of incident angles and positions. The first order peak of diffraction pattern was focused on the photodiode by a cylindrical lens. The position signal was normalized by total intensity of the peak. The diffraction pattern in air was usually less intense and more diffuse than that in solution. There are at least two reasons for this. The first one is that the muscle fiber itself scatters light as a short-focus cylindrical lens. The second reason is the light diffusion caused by a droplet of solution usually attached to the fiber surface. Despite these limitations, the sarcomere length signal in air was usually good enough to measure sarcomere length and in some cases even permitted to use it for feedback control. A switching circuit kindly provided by Prof. V. Lombardi and Dr. M. Irving was used for the sarcomere length or force feedback control.

Force transducer

A piezo-electric force transducer similar to that used before (Bershitsky and Tsaturyan, 1992) made from a commercial piezo crystal had a resonant frequency of approximately 15 kHz in both air and solution and a time constant of electric charge drain of 3 s. It was damped with a droplet of dimethylpolysiloxane (DMPS-1C; Sigma Chemical Co.). A slack test (~4% of fiber length) was applied to muscle fiber in the end of each frame to record the tension baseline.

Length motor

A loudspeaker-type servo motor was made with a Nd-Fe-B permanent ring magnet (Institute of Physics of Metals, Urals Branch of the Russian Academy of Sciences, Yekaterinburg, Russia). The moving part of the motor was a catalin (Catalin Ltd., Essex, UK) reel fixed with epoxy resin to a pivot made of three axially joined pieces of 1-mm-diameter carbon fiber rods (Goodfellow, Cambridge, UK). The moving part was stiff enough to provide step displacements up to ±50 μm within 0.12 ms with less then 5% overshoot. A 20-turn coil wound on the reel was made from 0.1-mm copper wire. An optical position sensor made of a 6-mW infrared light-emitting diode (AL-107A, Russia) and a quadrant photodiode (FD-K-142, Russia) had noise corresponding to 0.05-μm peak-to peak and a linear range of ±200 μm. The pivot ended by a half-cut nickel tube 0.3 mm in diameter where muscle fibers were glued. This tube was the active electrode of the T-jump device. A similar tube fixed on the force transducer was the ground electrode.

Recording and data analysis

Force, temperature, and total fiber length and sarcomere length changes were recorded with a 4-channel high speed data acquisition interface (DAS-50; Keithley MetraByte Corp., Taunton, MA) and then transferred onto the hard disk of a personal computer. The sampling rate was 50 or 100 kHz per channel. For data analysis, a licensed copy of Scientific Graphic Interactive Management System (GIM, versions 2.0–3.0; copyright by A. Drachev, Dr. Achey Development, Tempe, AZ) was used. The system allows multiexponential analysis of noisy curves using incorporated routine (Provencher, 1976) as well as computer simulation and graphics.

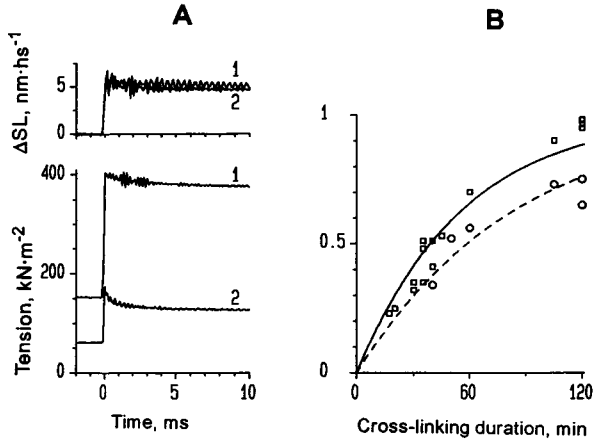

FIGURE 1 Stiffness of EDC-cross-linked fibers. (*A*) an example of experimental records. Changes of sarcomere length (upper traces) and tension (lower traces) after stretching of a fiber in rigor solution (*1*) and HSRS (*2*) after 35 min of cross-linking with 15 mM EDC. Sarcomere length, 2.5 μm; fiber dimensions, 1.96 mm × 4160 μm²; 5°C. (*B*): Stiffness in HSRS normalized for that in rigor, S_N, versus total duration of EDC cross-linking. □, fibers cross-linked with EDC continuously; ○, fibers for which EDC treatment was interrupted with two to three relaxations; —— and - - - -, exponential fittings for continuous and interrupted cross-linking, respectively.

RESULTS

EDC cross-linking

Extent of cross-linking was estimated by comparison of the instantaneous fiber stiffness in HSRS with that in rigor solution. In HSRS all unlinked myosin heads are detached from actin and only the cross-linked ones contribute to stiffness (Tawada and Kimura, 1986). For stiffness measurement, fibers were stretched by up to 5 nm per half-sarcomere (nm/hs) for 0.12 ms and tension and sarcomere length responses were recorded (Fig. 1 *A*). Stiffness was measured as the ratio of the amplitudes of the tension and the sarcomere length changes during the stretching. No corrections were done for dynamic properties of the force transducer, fast tension recovery, or inertia.

The EDC cross-linking led to a slight increase of rigor stiffness. The increase was roughly proportional to the cross-linking duration as reported by Tawada and Kimura (1986). However, when cyclic stretches and releases (see Materials and Methods) were applied during EDC treatment, this increase did not exceed 10% even after 2 h of cross-linking and was negligible after 20–40 min. When the ionic strength (IS) of the rigor solution was increased from 0.1 to 0.6 M, stiffness of the cross-linked fibers did not change. Rigor stiffness decreased with temperature with a coefficient of $-(7.5 \pm 2) \times 10^{-3}\ K^{-1}$, which is similar to that reported earlier (Bershitsky and Tsaturyan, 1986, 1989). Thus, a T-jump from 6–10°C to 30–40°C induced approximately a 20% decrease in rigor stiffness.

Before cross-linking, fiber stiffness at full activation at 5°C was 60–70% of rigor. The T-jump led to an increase in active stiffness by 25–30%, and at near physiological temperature of 35–38°C, the active stiffness achieved >90% of that in rigor at the same temperature. This indicates that almost all of the cross-bridges were attached to the thin filaments.

After cross-linking, fiber stiffness in an activating solution of 0.2 M IS was slightly less than that before EDC treatment. Relaxation in a 0.2 M IS solution led to a decrease in stiffness. Increasing the IS of relaxing solution to 0.6 M (HSRS) brought stiffness down to its lowest value, which depended on the extent of cross-linking. Inasmuch as additional elevation of the IS of the relaxing solution does not decrease stiffness (Tawada and Kimura, 1986), this limit was used for the estimation of the number of cross-bridges cross-linked to the thin filaments. Fiber stiffness in HSRS decreased with temperature with the same coefficient as in rigor. Thus, the ratio of stiffness in HSRS to that in rigor, S_N, is temperature independent and can be used as a measure of the cross-linking extent. Fig. 1 *B* shows S_N dependence on the duration of cross-linking. For continuous cross-linking with 15 mM EDC at 15°C, the half-time of stiffness rise was 40 ± 3 min (mean ± SD, Fig. 1 *B*). After 2 h of EDC treatment, S_N achieved 0.93–0.98, indicating that almost all of the cross-bridges were cross-linked. However, if the EDC treatment was interrupted by two to three fiber relaxations, the half-time increased to 60 ± 5 min (dashed line on Fig. 1 *B*) and S_N was ≤0.8 even after 2 h of total exposure to the EDC solution.

ATPase rate in EDC cross-linked fiber

In a control experiment, the ATPase rate after 30 min of EDC cross-linking (S_N = 32%) was measured in HSRS at 15°C. Release of Mg-ADP from a fiber segment of 10-nl volume into a 100-μl trough was 2.5×10^{-9} mol/h. Thus, the ATPase rate within the fiber was ~67 μM s^{-1}. Taking the concentration of myosin heads in a permeabilized rabbit fiber to be 154 μM (Ferenczi et al., 1984), one can estimate an ATPase rate of 0.45 s^{-1} per head. This value is 25–20% of that measured by Glyn and Sleep (1985) and Potma et al. (1994) during isometric contraction at 15°C (1.78 ± 0.24 s^{-1} and 2.3 ± 0.05 s^{-1}, respectively). At S_N = 32%, from 17 to 32% of the heads were cross-linked and able to interact with actin in HSRS. Quantitative estimation of the number of cross-linked heads depends on relative compliance of the structural elements within a sarcomere (see Discussion). Thus, ATPase activity per attached cross-bridge after the cross-linking was in the range of ±30% of that during normal isometric contraction. A contribution of unlinked heads to the ATPase activity in HSRS could not exceed 20% of total ATPase rate as, even at normal ionic strength, ATP hydrolysis by detached myosin heads is less than 0.1 s^{-1} (Ferenczi et al., 1984) and probably is less than 0.04 s^{-1} (Potma et al., 1994).

Mechanical responses in cross-linked fibers

As shown in Fig. 1 *A*, in rigor, a step length perturbation (L-step) induced an almost pure elastic response. Tension changed simultaneously with sarcomere length and the subsequent tension relaxation was small and slow. In contrast, after short-term cross-linking ($S_N \leq 0.4$), tension relaxation induced by the L-step in HSRS was much faster and more pronounced. This response is similar to the partial early tension recovery described by Huxley and Simmons (1971) in intact fibers. With an additional increase in the extent of cross-linking, the responses became more rigor-like. For this reason, we studied the mechanical properties of the partially cross-linked fibers where S_N was in the range of 0.25–0.4.

The main feature of the Huxley-Simmons transients is a dependence of the kinetics of the tension responses on the direction and magnitude of the length changes (Huxley and Simmons, 1971; Ford et al., 1977). To test whether the cross-bridges can produce Huxley-Simmons-like transients after cross-linking to actin, we studied the length dependence of the mechanical transients in the cross-linked fibers in HSRS. After a fiber was cross-linked, tension could be set arbitrarily by lengthening or shortening of the fiber. In mechanical experiments, we adjusted the fiber prestretch to scale tension with stiffness to obtain values close to those found in the fully activated fiber before cross-linking. Therefore, the average strain of cross-bridges in the cross-linked fiber was approximately the same as that during active contraction at a given temperature. Tension responses to the L-steps from +1.6 to −4 nm/hs at 5°C are shown in Fig. 2 *A*. The amount of partial tension recovery increased with the extent of fiber step shortening. Despite rather noisy records at low (100–150 μN) force level, the acceleration of the transients as the amplitude of the length release increases can be seen by eye (Fig. 2 *A*). The kinetics of the responses were complex but could be fitted reasonably well with a single exponential. The apparent rate constant, k_{app}, is shown against the amplitude of the length step in Fig. 2 *B*. This constant behaves in a Huxley-Simmons manner and is similar to that during contraction of unlinked fibers (Fig. 2 *B*). Of course, no slow final tension recovery (phase 4, Huxley and Simmons, 1971) is seen in cross-linked fibers in HSRS as cross-bridge reattachment is impossible (Fig. 2 *A*).

When temperature was increased from 5–10°C to 20–25°C, tension in HSRS increased approximately 1.5 times despite a slight decrease in stiffness. The fast partial tension recovery after the L-step was followed by a slow transient tension change in the opposite direction (Fig. 3). The kinetics of the tension responses were fitted by the sum of three exponentials by using Provencher's (1976) routine. The rate constants of the first (4,000–10,000 s^{-1}) and the second (400–1000 s^{-1}) components also increased with the release amplitude. The amplitude of the third exponential was too small for reliable analysis of its rate constant. It usually was in the range of 10–100 s^{-1} at 20–25°C.

Activation with 0.2 M IS solution (pCa ≤ 4.5) led to a further tension increase (Fig. 4) accompanied by a 1.5- to 2-fold stiffness enhancement. The fast partial tension recovery was in this case followed by a slow one, similar to that before cross-linking. The slow tension recovery caused by cycling of the unlinked myosin heads was incomplete as cross-linked heads that are unable to detach and reattach resisted this process. No significant change in the kinetics of

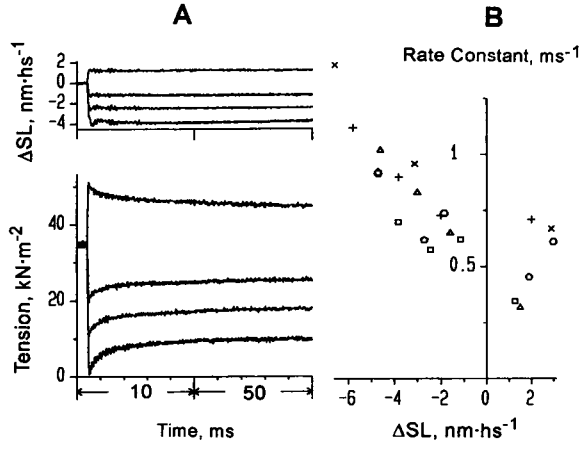

FIGURE 2 Mechanical responses to L-steps in EDC-cross-linked fibers in HSRS at 5°C. (*A*) Records of sarcomere length changes (*upper traces*) and tension (*lower traces*) after cross-linking for 20 min with 15 mM EDC. Sarcomere length, 2.55 μm; fiber dimensions, 1.92 mm × 6350 μm^2. (*B*) Dependence of the apparent rate constant of the fast partial tension recovery after the L-steps, k_{app}, on the size of the length step. Open symbols represent different cross-linked fibers in HSRS with S_N = 0.25–0.4; crosses represent unlinked fibers in the activating solution of 0.2 M IS.

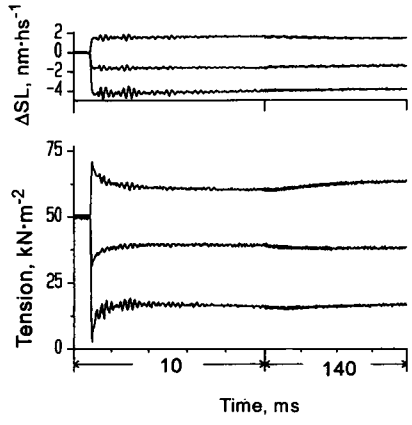

FIGURE 3 Responses of sarcomere length (*upper traces*) and tension (*lower traces*) to L-steps in HSRS at 20°C. The fiber was cross-linked with 15 mM EDC for 20 min; S_N = 0.25. Sarcomere length, 2.4 μm; fiber dimensions, 2.05 mm × 6400 μm².

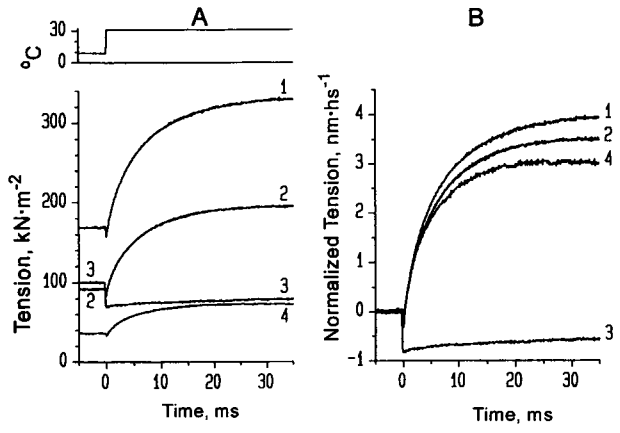

FIGURE 5 Tension responses to the T-jumps from 9°C to 28–31°C before (*1* and *3*) and after (*2* and *4*) EDC cross-linking for 20 min; S_N = 0.28. (*A*) Tension traces in the activating solution (*1* and *2*), rigor (*3*), and HSRS (*4*). (*B*) Same traces as in *A* but the tension change after the T-jump, Δ*T*, was normalized for fiber stiffness, *S*, in the same solutions at 30°C. Sarcomere length, 2.45 μm; fiber dimensions, 1.94 mm × 4600 μm².

the fast partial tension recovery was found in the activating solution compared with HSRS.

T-jump-induced responses in cross-linked fibers

In permeabilized Ca^{2+}-activated muscle fibers, high-amplitude T-jumps were shown to induce a severalfold tension rise accompanied by a slight increase in stiffness (Bershitsky and Tsaturyan, 1988, 1989, 1992). This approach was used to test the force-generating ability of the cross-linked cross-bridges. Fig. 4 *A* shows tension transients induced by T-jumps from 6–10°C to 28–31°C before and after the cross-linking. The T-jump in an activated fiber before cross-linking led to a twofold tension rise following an initial tension drop caused by thermal expansion (trace 1 in Fig. 5). Fiber stiffness also increased during the transient by ~25% and achieved 98% of the rigor stiffness at the plateau of the transient. In rigor, the T-jump caused only the tension drop (trace 3 in Fig. 5). The rigor responses did not change after cross-linking and were independent of ionic strength. In partially cross-linked fibers (S_N = 0.25–0.4), the T-jumps in HSRS initiated a tension rise similar to that before cross-linking (trace 4 in Fig. 5). With further extent of cross-linking, the fibers lost their force-generating ability and the tension transients after the T-jumps became more rigor-like.

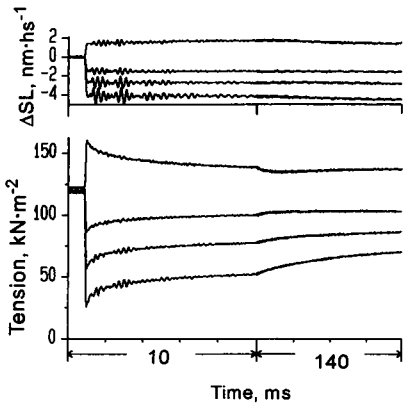

FIGURE 4 Responses of sarcomere length (*upper traces*) and tension (*lower traces*) to L-steps in the activating solution after EDC cross-linking (pCa = 4.5; IS = 0.2 M; 20°C). The fiber is the same as that in Fig. 3.

Transferring the partially cross-linked fiber (S_N = 0.25–0.4) from HSRS to an activating solution at 0.2 M IS caused an increase in both tension and stiffness (trace 2 in Fig. 5), which, however, never achieved their level before cross-linking. In HSRS, only cross-linked cross-bridges could contribute to the mechanical responses. An increase in stiffness and tension indicates that a substantial number of unlinked cross-bridges were recruited for interaction between thin and thick filaments in the activating solution. The amplitude of the T-jump-induced transients in the activating solution also increased compared with those in HSRS, although these were less pronounced than before cross-linking (Fig. 5).

To compare the tension transients involving different numbers of cross-bridges, tension changes after the T-jump were normalized for fiber stiffness at their final temperature. The normalized traces are shown in Fig. 5 *B*. It is seen that in the presence of ATP the normalized responses in the cross-linked fiber were similar to those before cross-linking. In HSRS, the kinetics of tension rise were slightly faster compared with those before cross-linking. In activating solution, both the amplitude and the kinetics were intermediate. In any case, the kinetics of the T-jump-induced transients were much slower than those of the L-step-induced transients.

To minimize possible effects of prestretching of the cross-linked fibers, the dependence of the T-jump-induced

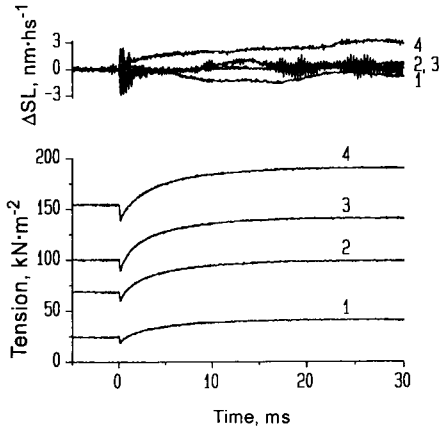

FIGURE 6 Responses of sarcomere length (*upper traces*) and tension (*lower traces*) to the T-jumps from 10°C to 37.5–38.5°C applied at zero time at different degrees of prestretch. A fiber was cross-linked with EDC for 30 min and then immersed in HSRS; S_N = 0.28. Sarcomere length, 2.5 μm; fiber dimensions, 1.84 mm × 4200 μm^2.

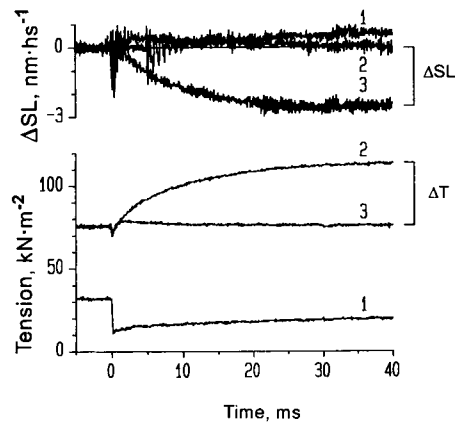

FIGURE 8 Sarcomere length (*upper traces*) and tension (*lower traces*) responses to the T-jumps from 10°C to 32.1–32.5°C applied at zero time under total length (*1* and *2*) and force (*3*) feedback control. A fiber was cross-linked with EDC for 40 min and then immersed in rigor solution (*1*) or HSRS (*2* and *3*); S_N = 0.34. Sarcomere length, 2.5 μm; fiber dimensions, 1.96 mm × 4160 μm^2. Bars show sarcomere shortening (ΔSL = 2.6 nm hs^{-1}) at constant force and tension rise (ΔT = 38 kN m^{-2}) at constant sarcomere length.

transients on the initial tension was studied in a control experiment. Fig. 6 shows tension and sarcomere length transients in HSRS after T-jumps from 10°C to 37–38.5°C at different fiber prestretch lengths. Its optimal range was found when sarcomere length was near constant during the tension rise. In this case, the amplitude of the rise was maximal (traces 2 and 3 in Fig. 6). Outside of this range, sarcomeres shortened or elongated and the tension increase was less pronounced. The kinetics of the tension rise were fitted by a single exponential the rate constant (250–300 s^{-1}) of which was independent of the prestretch (Fig. 7 *B*). At the optimal length, the tension-to-stiffness ratio was 1.2–1.5 of that during contraction at 5–6°C before cross-linking. Thus, in the T-jump experiments we adjusted the fiber length to be at this optimal level.

To test the ability of the cross-linked cross-bridges to shorten, the feedback force control was used during the T-jump-induced transients in HSRS. The records of tension and sarcomere length under force control are superimposed to those under isometric conditions in Fig. 8. It is seen that tension rise of 38 kN m^{-2} could be compensated by a 2.6-nm/hs shortening. This shortening has the same time course as the tension rise. The same shortening value, ΔSL = 2.6 nm/hs, could be found by dividing the tension rise amplitude, ΔT = 38 kN m^{-2}, by the fiber stiffness, S = 15 × 10^{12} N hs m^{-3}, at 30°C. Thus, the amplitude of the tension rise normalized for the fiber stiffness indeed characterizes the shortening ability of the cross-linked cross-bridges.

Fig. 9 shows the normalized tension rise in response to

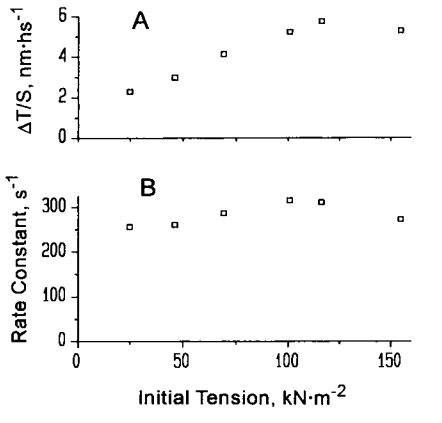

FIGURE 7 (*A*) Amplitude of the tension rise (ΔT = steady-state tension after the T-jump minus its minimal level just after the T-jump) normalized for fiber stiffness, *S*. (*B*) Rate constant of the tension rise as a function of initial tension. Data were obtained from the experiment presented in Fig. 6.

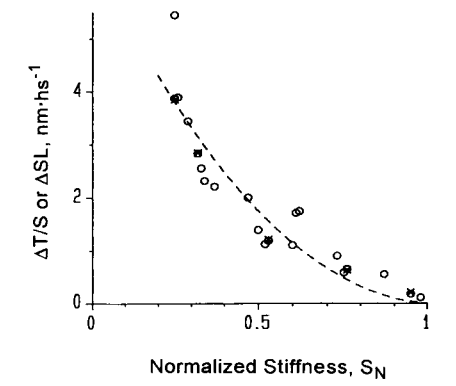

FIGURE 9 Sarcomere shortening (ΔSL, ×) or tension rise (ΔT, normalized for stiffness, *S*; ○) versus extent of cross-linking estimated as fiber stiffness in HSRS normalized for that in rigor solution, S_N.

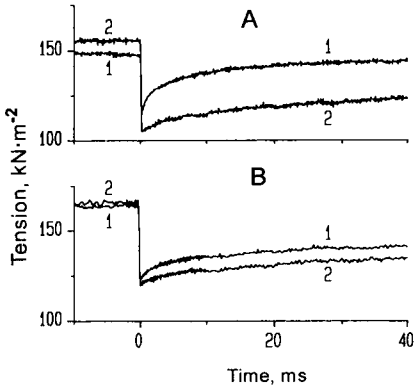

FIGURE 10 Tension responses to T-jumps from 10°C to 32–35°C applied at zero time in HSRS (*1*) and rigor solution (*2*). (*A*) Fiber was cross-linked as follows. After EDC treatment for 30 min, EDC was washed out and fiber was relaxed with HSRS. This procedure was repeated four times to get a total EDC exposure of 120 min (S_N = 0.75). Sarcomere length, 2.5 μm; fiber dimensions, 1.96 mm × 4100 μm^2. (*B*) Fiber was cross-linked with EDC for 120 min continuously (S_N = 0.95). Sarcomere length, 2.5 μm; fiber dimensions, 1.64 mm × 6700 μm^2.

the T-jump against the normalized stiffness, S_N. It is obvious that the ability to produce tension and shortening decreases with the extent of cross-linking. When S_N was >90%, the responses were very similar to rigor ones (Fig. 10). To distinguish whether the loss of the force-generating ability is caused by the extent of the cross-bridge cross-linking itself and not by any side effects of a long-term EDC treatment, we compared the responses after 120 min of continuous cross-linking with those after cross-linking for four times for 30 min each. As is seen in Fig. 10, cross-linking interrupted by the fiber relaxations led to a relative decrease in S_N. Data presented in Fig. 10 show that despite the same total EDC exposure, the tension rise after the T-jump was significantly more pronounced after the interrupted cross-linking. In this case, the normalized tension rise was rather similar to that after 60 min of continuous EDC treatment.

DISCUSSION

EDC cross-linking

In solutions of F-actin and myosin subfragment-1 (S-1), EDC zero-length cross-linking was used as a tool for studying acto-myosin interaction. It was shown that EDC cross-links actin to S-1 stoichiometrically (Sutoh, 1983; Heaphy and Tregear, 1984). Only carboxyl groups of actin (Glu and/or Asp) could be cross-linked to amino group(s) of S-1 (most probably, Lys), not inversely (Mornet et al., 1981). Cross-linking involves the amino-terminal region (residues 1–12) of actin (Sutoh, 1982; Bertrand et al., 1988; Combeau et al., 1992) and the lysine-rich 50- to 20-K junction in S-1. In the high-resolution spatial structure of the acto-myosin complex (Rayment et al., 1993a), localization of this bond corresponds to a region of nonspecific electrostatic interaction that, most probably, is responsible for weak binding. It is, however, difficult to determine which particular amino acids can participate in cross-linking with EDC, as the lysine-rich loop (residues 627–646) is disordered in the S-1 crystals (Rayment et al., 1993b).

EDC cross-linking permits S-1 to alternate between weak and strong binding conformations. When Mg-ATP is added to cross-linked acto-S-1, electron microscopy shows a broad angle distribution of S-1 with respect to the axis of the actin filament, in contrast to the arrowhead structures seen in rigor (Craig et al., 1985). Mobility of S-1 on the microsecond time scale also appears when ATP is added to cross-linked acto-S-1, as determined from electron paramagnetic resonance spectra (Svensson and Thomas, 1986). This microsecond rotational motion of EDC-cross-linked S-1 is similar to that of unlinked heads attached to actin in solution (Berger et al., 1989) and in myofibrils (Berger and Thomas, 1993). The ability of cross-linked S-1 to affect the troponin-tropomyosin-actin complex can also be modified by transition from weak to strong binding states (King and Greene, 1987).

The ATPase rate of cross-linked acto-S-1 is close to that of the unlinked complex at saturating actin concentration (Mornet et al., 1981; Brenner and Eisenberg, 1986; King and Greene, 1987) and does not decrease at IS up to 0.6 M (Huang et al., 1990). Our control experiment showed that in muscle fibers the ATPase rate of cross-linked acto-myosin is also close to that during an active isometric contraction (Glyn and Sleep, 1985; Potma et al., 1994).

In muscle fibers and myofibrils, EDC was shown to cross-link myosin heads to the actin filaments as well as to induce cross-linking within the myosin rods (Tawada and Kimura, 1986; Duong and Reisler, 1989; Herrmann et al., 1993). This latter point enables us to increase the IS up to 1 M without dissolving the myosin rods. In HSRS of 0.6 M IS all unlinked heads are detached from actin and stiffness can then be used as a measure of the extent of cross-linking (Tawada and Kimura, 1986). In a control experiment, addition of 50 mM 2,3-butanedione monoxime (Horiuti et al., 1988) and 20 mM inorganic phosphate to HSRS did not lead to a further decrease of fiber stiffness. The cross-linking kinetics estimated by stiffness presented in Fig. 1 is consistent with that reported by Tawada and Kimura (1986), taking into account the difference in temperature and EDC concentration.

Inactivation of myosin heads by EDC cross-linking

Cross-linking with EDC led to a decrease of force-generating ability of both unlinked and cross-linked myosin heads.

When the EDC-cross-linked fiber was activated at 0.2 M IS, active force and stiffness were less than those before the cross-linking. Data presented by Tawada and Kimura (1986, Fig. 4) also show incomplete activation after EDC cross-

linking. This suppression of force-generating ability increased progressively with the extent of the cross-linking. This effect can hardly be explained by cross-linking of S-1 or S-2 to the backbone of the thick filaments because rigor stiffness never decreased after EDC cross-linking even for 120 min. Thus, only the ability of unlinked myosin heads to bind actin weakly suffered after EDC treatment whereas strong interaction was preserved even at high IS. A possible explanation for this is the EDC cross-linking of the actin amino terminal to another actin monomer or to tropomyosin and to troponin-I (Grabarek and Gergely, 1990). If only carboxyls responsible for the weak electrostatic interaction with myosin were involved in this side cross-linking, stereospecific strong binding should remain unaffected. Evidence for this explanation is presented in Fig. 1 *B*. If EDC treatment was interrupted by relaxations with HSRS, the cross-linking kinetics was decelerated and S_N was $\leq 75\%$ even after 120 min of total EDC exposure. In rigor, only approximately one-third of actin sites are occupied by myosin heads whereas the rest of actin monomers may be cross-linked to their neighbors or regulatory proteins. If, after the relaxation, unlinked heads reattach in rigor to these spoiled actin sites, they cannot be cross-linked anymore. In a control experiment, EDC cross-linking was carried out in the presence of 50 mM 2,3-butanedione monoxime, 20 mM inorganic phosphate (P_i), and 5 mM Mg-ATP to check for the effect of EDC on the actin monomers unprotected by the myosin heads. After 15 min of treatment with 10 mM EDC, stiffness in HSRS was less than 5% of that in rigor, but active tension at 0.2 M IS was only one-third of that before the cross-linking.

When cross-linking extent was increased and S_N reached 0.95, the mechanical properties of the fiber in HSRS became rigor-like. Neither tension relaxation after the L-steps nor tension rise after the T-jumps were observed. This indicates that EDC treatment inactivates some myosin heads cross-linked to actin. This could be caused by side reactions occurring during long-term EDC treatment. Data shown in Fig. 10 shows, however, that the rigor-like mechanical behavior correlates with S_N (and, therefore, p) rather than with the total duration of EDC treatment. Another possibility is that, if the two heads of a myosin molecule are cross-linked to actin, they lose their rotational ability because geometrical restrictions whereas cross-bridges cross-linked with only one head are active and able to produce L-step and T-jump transients. This assumption is in good agreement with experiments of Huang et al. (1990) who demonstrated that ATPase activity of EDC-cross-linked acto-heavy meromyosin can be increased twofold after converting acto-heavy meromyosin into acto-S-1 with chymotrypsin. If it is true and the myosin head can produce the force-generating step only when its neighbor is detached from actin, then the two heads should step alternately, like a pair of legs.

After partial cross-linking, when S_N = 25–40%, some cross-linked myosin heads were probably also inactivated. Their contribution to mechanical responses was not, however, significant. As is seen from Fig. 5 *B*, the amplitude of the tension rise after the T-jump in HSRS normalized for stiffness was approximately 75% of that during activation before the cross-linking. This means that less than 25% of the force generators were inactivated at $S_N = 28\%$, because stiffness gives the highest estimation of the number of cross-linked heads (see below).

Stiffness as a measure of the extent of cross-linking

Tawada and Kimura (1986) have shown that in a muscle fiber EDC cross-links two heads of a myosin molecule independently. This means that the probability of the cross-bridge cross-linking with both heads is p^2 and probability of cross-linking with only one head is $2p(1 - p)$ where p is the cross-linking extent or the probability of cross-linking of a myosin head. Quantitative estimation of p using stiffness measurements is model dependent. There are two unknown parameters that should be specified in a quantitative model. The first one is the compliance of the thin and thick filaments, C_f, compared with that of the cross-bridges C_{cb}. The estimates made by Ford et al. (1981) that during isometric contraction $C_f/C_{cb} \leq 0.1$ are probably not quite correct. Recent x-ray data (Huxley et al., 1994; Wakabayashi et al., 1994) show that $C_f/C_{cb} \approx 1$, suggesting that the filaments are as compliant as the cross-bridges. Another unknown parameter is the localization of the elastic element within a cross-bridge. If each head has its own elastic element, the stiffness of the cross-bridges in HSRS normalized for that in rigor is $S_{cb} = p$. If the two heads share one elastic element, $S_{cb} = p(2 - p)$. Fig. 11 shows the relationship between cross-linking extent, p, and stiffness of a half-sarcomere normalized for that in rigor, S_N, for different models of the cross-bridge and filament stiffness. Calculations were made

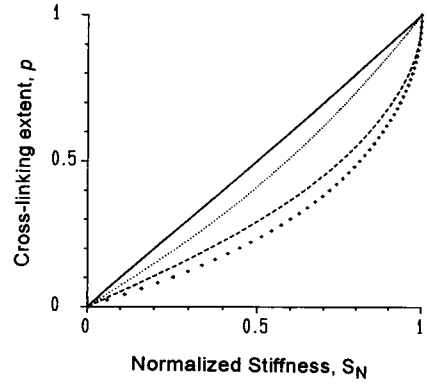

FIGURE 11 Model calculations of the relationship between fiber stiffness in HSRS normalized for that in rigor, S_N, and the extent of cross-linking, p. ——, $C_f/C_{cb} = 0$ (each myosin head has its own elastic element); - - - - -, $C_f/C_{cb} = 0$ (two heads of a myosin molecule share an elastic element); · · · · ·, $C_f/C_{cb} = 1$ (own elastic element); + + + +, $C_f/C_{cb} = 1$ (shared elastic element).

using the theory of Ford et al. (1981). It is seen that the relationship is markedly different for the different models. At partial cross-linking, S_N was 0.25–0.4 and cross-linking extent, p, was somewhere between 0.1 and 0.4. Independently of the localization of the elastic element and the filament compliance, most of the cross-bridges were, in this case, cross-linked with only one head, whereas at $S_N > 0.9$ almost all of them were cross-linked with both heads.

Mechanical responses in cross-linked fibers

Cross-linked fibers are very stable. They survive up to 50 activation/relaxation cycles and high-amplitude T-jumps and can be activated with a solution of 0.2 M IS at room temperature for several minutes without losing tension, stiffness, or the quality of the sarcomere length signal.

Muscle fibers partially cross-linked with EDC were shown to produce work in HSRS during small amplitude (0.125%) sine oscillations of fiber length (Tawada and Kawai, 1990). These fibers also generated some force upon transfer from HSRS to rigor solution (Tawada et al., 1989). Here we show that, after partial cross-linking, tension responses to step length changes in HSRS are similar to the fast components of the mechanical transients during normal isometric contraction (Figs. 2 and 3). As described by Huxley and Simmons (1971) in intact fully activated muscle fibers, the elastic response during the L-step is followed by a fast partial tension recovery the kinetics of which accelerate with the amplitude of the length step release of the fiber. Data shown in Fig. 2 were obtained in conditions where only cross-linked myosin heads participate in the mechanical responses. Their similarity to the Huxley-Simmons transients is strong evidence that the fast components of the tension responses occur by some conformational change in the attached cross-bridges, not by their detachment and reattachment (Huxley and Simmons, 1971).

When the temperature of EDC-cross-linked fibers in HSRS is increased to >20°C, a fast partial tension recovery is followed by a small-amplitude slow tension change in the reverse direction (Fig. 3). Such a behavior resembles phase 3 of Huxley-Simmons transients (Huxley and Simmons, 1971). In our experiments, however, the slow tension change was not accompanied by any change in stiffness, whereas in unlinked fibers there is a transitory stiffness decrease during phase 3 (Iino and Simmons, 1982; Lombardi et al., 1992). This indicates that slow tension changes in cross-linked fibers reflect some process in cross-bridges. This process is responsible for work production during sinusoidal length oscillation of the cross-linked fibers (Tawada and Kawai, 1990).

T-jump-induced responses in cross-linked fibers

Here we show that a high-amplitude T-jump induces force generation or shortening produced exclusively by covalently cross-linked cross-bridges. The T-jump-induced tension rise normalized for stiffness was used as a quantitative measure of the force-generating ability of the cross-bridges. At optimal prestretch, the normalized tension rise in HSRS was slightly lower and faster than that during activation before cross-linking (Fig. 5 *B*). An acceleration of the kinetics (Fig. 5 *B*) can be explained by the fact that cross-bridge reattachment was excluded in cross-linked fibers in HSRS. In unlinked fibers, the reattachment was shown to participate in mechanical responses to the T-jump (Bershitsky and Tsaturyan, 1992). The apparent rate constant of the T-jump-induced tension rise was 200–300 s^{-1} at 30–38°C.

Cross-linked cross-bridges produce shortening after the T-jump at constant force (Fig. 8). After partial cross-linking (S_N = 0.25–0.4), observed shortening was up to 4 nm per half-sarcomere and was quantitatively estimated in isometric conditions by the amplitude of the tension rise normalized for stiffness (Figs. 8 and 9). The calculated shortening was up to 5.5 nm (Fig. 7 *A*). Both values, 4 and 5.5 nm, give a rather underestimated amplitude of the cross-bridge step. First, some cross-linked cross-bridges do not undergo the shortening-producing step and therefore resist shortening. The portion of the shortening-resistant cross-bridges increases with the extent of cross-linking (Fig. 9), but their number can be substantial even at low S_N. Second, in our experiments, cross-bridges produced shortening under a significant load comparable with that during isometric contraction. Taking these factors into account, we consider our data to be consistent with a step size of 11–15 nm estimated in the in vitro motility assay (Finer et al., 1994).

The bearing force and work produced by a cross-linked cross-bridge after the T-jump can be estimated as follows. At partial cross-linking, S_N was 0.25–0.4 and cross-linking extent P = 0.1–0.4 (Fig. 11). Tension before the T-jump at optimal prestretch was 40–100 kN/m^2. Taking a sarcomere length of 2.4 μm and a concentration of myosin heads in a fiber as 150 μM (Ferenczi et al., 1984), the estimate of force per cross-linked myosin head is 1.5–2.5 pN, if thin and thick filaments are rigid and each head has its own elastic element, or 4–5.5 pN if $C_f/C_{cb} = 1$ and the two heads share an elastic element. Multiplying this force by the 4- to 5.5-nm shortening of a half-sarcomere, one can calculate the work to be $6.5–30 \times 10^{-21}$ J or 1.6–7.5 kT (where k is the Boltzman's constant and T is the absolute temperature) produced by a myosin head after a T-jump at optimal prestretch.

Most probably, not all cross-linked myosin heads are involved in the mechanical responses to the T-jump and the extensibility of the filaments is not negligible. Thus, the cross-bridge work is probably close to the upper value above of 5–7.5 kT. This means that an endothermic process responsible for the mechanical transients induced by the T-jump is associated with substantial work production. This work is a significant portion of the total free energy of the ATP hydrolysis (90×10^{-21} J or 22 kT).

The most surprising feature of transients shown in Fig. 6 is the independence of the kinetics of the tension rise on the prestretch level. The rate constant changed by ≤20% when the initial tension increased sixfold and work rose from near zero to 5 kT (Fig. 7). We cannot give any reasonable account for this result, but it probably cannot be explained within a framework of existing models based on the theory of absolute reaction rates (Huxley and Simmons, 1971). According to these models, the rate constant of the force-generating process is an exponential function of the cross-bridge work normalized for kT and this rate constant should change 2.7-fold when work produced by a cross-bridge changes by 1 $kT = 4 \times 10^{-21}$ J. Calculations taking into account the difference in positions of the myosin heads relative to the nearest suitably oriented actin (Goldman and Huxley, 1994) show that the kinetics of the averaged response of the cross-bridges could be less strain dependent than predicted by the original theory of Huxley and Simmons (1971) but probably still more strain dependent than we observed here.

We thank the Wellcome Trust for fellowships. We are grateful to Prof. R. M. Simmons, Drs. M. Irving, and J. A. Sleep for fruitful discussions and Dr. M. A. Ferenczi for helpful comments on the manuscript. We are also grateful to Prof. V. Lombardi and Dr. K. Burton for providing parts of the experimental set-up and to Mr. P. Stoneham, Mr. B. McCarthy, and Mr. K. Eston for technical assistance.

REFERENCES

Berger, C. L., E. C. Svensson, and D. D. Thomas 1989. Photolysis of a photolabile precursor of ATP (caged ATP) induces microsecond rotational motions of myosin heads bound to actin. *Proc. Natl. Acad. Sci. USA.* 86:8753–8757.

Berger, C. L., and D. D. Thomas. 1993. Rotational dynamics of actin-bound myosin heads in active myofibrils. *Biochemistry.* 32:3812–3821.

Bershitsky, S. Y., and A. K. Tsaturyan. 1986. Thermoelastic properties of the cross-bridges in permeabilized muscle fibers of the frog in rigor state. *Biophysics (Engl. Transl. Biofizika).* 31:532–533.

Bershitsky, S. Y., and A. K. Tsaturyan. 1988. Biphasic tension response to the temperature jump in the Ca^{2+} activated frog skeletal muscle fibers. *Biophysics (Engl. Transl. Biofizika).* 33:156–158.

Bershitsky, S. Y., and A. K. Tsaturyan. 1989. Effect of joule temperature jump on tension and stiffness of permeabilized rabbit muscle fibers. *Biophys. J.* 56:809–816.

Bershitsky, S. Y., and A. K. Tsaturyan. 1992. Tension responses to joule temperature jump in permeabilized rabbit muscle fibers. *J. Physiol.* 447:425–448.

Bertrand, R., P. Chaussepied, E. Audemard, and R. Kassab. 1989. Functional characterization of skeletal F-actin labeled on the NH_2-terminal segment of residues 1–28. *Eur. J. Biochem.* 181:747–754.

Bertrand, R., P. Chaussepied, R. Kassab, M. Boyer, C. Roustan, and Y. Benyamin. 1988. Cross-linking of the skeletal myosin subfragment 1 heavy chain to the *N*-terminal actin segment of resides 40–113. *Biochemistry.* 27:5728–5736.

Brenner, B., and E. Eisenberg. 1986. Rate of force generation in muscle: correlation with actomyosin ATPase activity in solution. *Proc. Natl. Acad. Sci. USA.* 83:3542–3546.

Combeau, C., D. Didry, and M.-F. Carlier. 1992. Interaction between G-actin and myosin subfragment-1 probed by covalent cross-linking. *J. Biol. Chem.* 267:14038–14046.

Craig, R., L. E. Greene, and E. Eisenberg. 1985. Structure of the actin-myosin complex produced by crosslinking in the presence of ATP. *Proc. Natl. Acad. Sci. USA.* 82:3247–3251.

Duong A. M., and E. Reisler. 1989. Binding of myosin to actin in myofibrils during ATP hydrolysis. *Biochemistry.* 28:1307–1313.

Ferenczi, M. A., E. Homsher, E., and D. R. Trentham. 1984. The kinetics of magnesium adenosine triphosphate cleavage in permeabilized muscle fibers of the rabbit. *J. Physiol.* 352:575–599.

Finer, J. T., R. M. Simmons, and J. A. Spudich. 1994. Single myosin molecule mechanics: piconewton forces and nanometre steps. *Nature.* 368:113–119.

Ford, L. E., A. F. Huxley, and R. M. Simmons. 1977. Tension responses to sudden length change in stimulated frog muscle fibers near slack length. *J. Physiol.* 269:441–515.

Ford, L. E., A. F. Huxley, and R. M. Simmons. 1981. The relation between stiffness and filament overlap in stimulated frog muscle fibers. *J. Physiol.* 311:219–249.

Glyn, H., and J. Sleep. 1985. Dependence of adenosine triphosphate activity of rabbit psoas muscle fibres and myofibrils on substrate concentration. *J. Physiol. Lond.* 365:259–276.

Goldman, Y. E., and A. F. Huxley. 1994. Actin compliance: are you pulling my chain? *Biophys. J.* 67:2131–2136.

Grabarek, Z., and J. Gergely. 1990. Zero-length crosslinking procedure with the use of active esters. *Anal. Biochem.* 185:131–135.

Heaphy, S., and R. Tregear. 1984. Stoichiometry of covalent actin-subfragment 1 complexes formed on reaction with a zero-length cross-linking compound. *Biochemistry.* 23:2211–2214.

Herrmann, C., J. Sleep, P. Chaussepied, F. Travers, and T. Barman. 1993. A structural and kinetic study on myofibrils prevented from shortening by chemical cross-linking. *Biochemistry.* 32:7255–7263.

Horiuti, K., H. Higuchi, Y. Umazume, M. Konishi, O. Okazaki, and S. Kurihara. 1988. Mechanism of action of 2,3-butanedione 2-monoxime on contraction of frog skeletal muscle fibres. *J. Muscle Res. Cell Motil.* 9:156–164.

Huang, Y.-P., M. Kimura, and K. Tawada. 1990. Covalent crosslinking of myosin subfragment-1 and heavy meromyosin to actin at various molar ratios: different correlations between ATPase activity and crosslinking extent. *J. Muscle Res. Cell Motil.* 11:313–322.

Huxley, A. F., and R. M. Simmons. 1971. Proposed mechanism of force generation in striated muscle. *Nature.* 233:533–538.

Huxley, H. E., A. Stewart, H. Sosa, and T. Irving. 1994. X-ray diffraction measurements of the extensibility of actin and myosin filaments during muscle contraction. *Biophys. J.* 67:2411–2421.

Iino, M., and R. M. Simmons. 1982. Tension responses to double step length changes in frog permeabilized muscle fibers. *J. Physiol.* 332: 54P–55P.

Irving, M., V. Lombardi, M. A. Ferenczi, and G. Piazzesi. 1992. Myosin head movements are synchronous with the elementary force-generating process in muscle. *Nature.* 357:156–158.

King, R. T., and L. E. Greene. 1987. The conformation of cross-linked actin·S-1 in the presence and absence of ATP. *J. Biol. Chem.* 262: 6128–6134.

Lombardi, V., G. Piazzesi, and M. Linari. 1992. Rapid regeneration of the actin-myosin power stroke in contracting muscle. *Nature.* 355:638–641.

Mornet, D., R. Bertrand, P. Pantel, E. Audemard, and R. Kassab. 1981. Structure of the actin-myosin interface. *Nature.* 292:301–306.

Potma, E. J., G. J. M.Stienen, J. P. F. Barends, and G. Elsinga. 1994. Myofibrillar ATPase activity and mechanical performance of skinned fibres from rabbit psoas muscle. *J. Physiol.* 472:303–317.

Provencher, S. W. 1976. A Fourier method for the analysis of exponential decay curves. *Biophys. J.* 16:27–50.

Rayment, I., H. M. Holden, M. Whittaker, C. B. Yohn, M. Lorenz, K. C. Holmes, and R. A. Milligan. 1993a. Structure of the actin-myosin complex and its implication for muscle contraction. *Science.* 261: 58–65.

Rayment, I., W. R. Rypniewski, K. Schmidt-Base, R. Smith, D. R. Tomchick, M. M. Benning, D. A. Winkelmann, G. Wesenberg, and H. M. Holden. 1993b. Three-dimensional structure of myosin subfragment-1: a molecular motor. *Science.* 261:50–58.

Sutoh, K. 1982. Identification of myosin-binding sites on the actin sequence. *Biochemistry.* 21:3654–3661.

Sutoh, K. 1983. Mapping of actin-binding sites on the heavy chain of myosin subfragment 1. *Biochemistry.* 22:1579–1585.

Svensson, E. C., and D. D. Thomas. 1986. ATP induced microsecond rotational motions of myosin heads cross-linked to actin. *Biophys. J.* 50:999–1002.

Tawada, K., Y.-P. Huang, and Y. Emoto. 1989. Force production by covalently fixed cross-bridge heads in permeabilized fibers. *In* Muscle Energetics. Alan R. Liss, New York. 37–43.

Tawada, K., and M. Kawai. 1990. Covalent cross-linking of single fibers from rabbit psoas increases oscillatory power. *Biophys. J.* 57:643–647.

Tawada, K., and M. Kimura. 1986. Stiffness of carbodiimide-crosslinked glycerinated muscle fibers in rigor and relaxing solutions at high salt concentrations. *J. Muscle Res. Cell Motil.* 7:339–350.

Wakabayashi, K., Y. Sudimoto, H. Tanaka, Y. Ueno, Y. Takezawa, and Y. Amemiya. 1994. X-ray diffraction evidence for the extensibility of actin and myosin filaments during muscle contraction. *Biophys. J.* 67: 2422–2435.